Effect of Hartmann number on Natural Convection of Pleural Effusion

T. Padmavathi*1 and Dr. S. Senthamil Selvi2

- 1. Research Scholar, Department of Mathematics, VISTAS, Vels University, Pallavaram, Tamilnadu, India. (pathumyanmar@gmail.com)
- 2. Research Supervisor, Department of Mathematics, VISTAS, Vels University, Pallavaram, Tamilnadu, India.

Article History: Received: 10 January 2021; Revised: 12 February 2021; Accepted: 27 March 2021; Published online: 28 April 2021

Article History: Received: 10 January 2021; Revised: 12 February 2021; Accepted: 27 March 2021; Published online: 28 April 2021

ABSTRACT: The most severe pandemic complications of COVID-19 are mainly caused by large droplet transmission. An initial sign of coronavirus disease is pleural effusion. Droplet transmission of the COVID-19 virus can occur by direct contact with inflamed human beings and indirect touch with surrounding surfaces or with objects used by inflamed person. Present study describes the underlying physics of the pleural fluid deformation in the lung on free convection. Pleural effusion (excess fluid)happens whilst fluid strengthenthe area surrounded by the chest wall and lung, the tissue around the lung may become inflamed, this can manifest for plenty distinct speculate, such as pneumonia. The various velocity, temperature, concentration profiles are graphically obtained with increasing and decreasing non-dimensional parameter according to the nature of the pleural fluid.

Key words: COVID-19, Hartmann number, Natural Convection, Pleural fluid, Pleural effusion.

1. INTRODUCTION

In many years droplet ailment transmission has usually been a subject of extensive interest in numerous fields. The transposal of microbes and aggressivemicroorganism from extinct surfaces by affected men and women is a problem with reference to highly poisonous COVID-19 ailment transportation. The airbornetransmittal disorder begins while the infectious delegate which includes the influenza, COVID-19 or SARS viruses are exhaled from an inflamed individual. The procedure of transference is arbitrating with aid of complication go with the flow phenomena, length from air—mucous interplay, during evaporation it acts faster to settled down their big droplet length, it makes circumference pollution to the surfaces. Droplets are smaller than for this reason period evaporate quicker than they reach the position.

The primary function of the respiratory tract is gas exchange. The breathing tract carries extensive variety of micro-organisms. Contaminants of pleural fluid migrate through a respiratory tract. The complete breathing tract is continuously exposed to air, the general public of particles are wiped clean out by means of inhalation, however aspiration and mucosal and haematogenous unfold additionally arise. Individuals with healthy lungs hardly ever have any bacterial or virus contamination as particular surface antigens that adhere to mucosal epithelial cells.

A pleural effusion approach that there is an excess build-up of fluid between human lung and the chest wall. Every of our human lungs are surrounded by using pleura. The pleura is a thin membrane that lines the interior of the chest wall and display screen the lungs. There is generally a slight quantity of fluid among the two layers of pleura occupied. This acts like lubricating oil between the lungs and the chest wall as they circulate whilst we breathe. There are numerous varieties of pleural effusion induced with one-of-a-kind treatment followed by way of Transudative pleural effusion is brought on because of fluid leaking into the pleural area improved stress within the blood vessels, heart failure or a low blood protein. Exudative pleural effusion is as a result of hold up blood vessels or infections, tumours, pneumonia.

The complete quantity of human's pleural liquid in degrees between 0.13–0.27 mL kg^{-2/3}. As currently decided with the aid of urea mixture in topics go through thoracoscopy for remedy of hydropathic hyperhidrosis, is 0.26 mL kg⁻¹. The protein awareness in pleural fluid and their ratio during capillary plasma are low, it's already reported that the proteinof the pleurapermeability ought to be small. Generally, 1,700 cells·mm⁻³ were newly deduct in human normal pleural fluid ranges may vary by (75% macrophages, 23% lymphocytes, and 1% mesothelial cells) [1].

In lots of hospitals lately, the spread of respiration infection from recognised cases of influenza and pneumonia may be avoided with the aid of infection control strategies. These are called 'extra safety'. Warmness and mass switch in MHD flows arises in some of the technological applications. Operating fluids may be either Newtonian or non-Newtonian. inside the study of natural convection via porous media, the majority of the studies attempt has been committed to the flow resulting from a buoyancy impact of Temperature and Concentration variations. Flows induced with the aid of buoyancy consequences of thermal diffusion is detect often in motion of infections in the human respiration tract. Zahra Ahmadinejad. et al [1] discovered differential diagnosis of affected person under gone throughdyspnoea and dry cough referred to lung cancer and treated for

the COVID-19 infection.Saffman.P.G. [2] concerned with the effects of coarse and excellent dirt additionally investigated affectness of the critical Reynolds quantity for transition from laminar to turbulent go with the flow.Adrian Bejan.et al [3] summarized the buoyancy ratio and the Lewis variety simultaneously more than one scale boundary-layer trouble showed the effectivness of the order-of-importance measuremade via ratio test.

R. Mittal.et al [4] has tried to manifested glide physics of pandemic COVID-19 consisting of respiratory droplet formation, droplet evaporation. S. Das. et al [5] here The RosselandDiffusion Approximation defined the radiative warmth fluctuation in the potential equation. Alimitless vertical perpendicular plate with warmness and mass switch within the existence of thermal radiation had been concluded the use the method of Laplace transform. Christian J. et al [6] measured and identified nonlinear compressible simulations of lung parenchyma in different computational lung models. Experiments are compared with aggregate lung to permit the model named as vivo validation. Richard Haber et al [7] manifested the right fluid dynamic forces on the lung that counterbalance buoyancy and allow steady states of dis-association bounded by the pleura. Simultaneously the lung's buoyancybalanced by enlarged pressure in the pleural fluid.G. V. Ramana Reddy.et al [8] explored an unsteady free convective mass transfer flow past an infinite vertical plate with variable suction velocity in the presence of Soret effects and MHD effects .T. B. Martonen et al. [9] described and model developed for several conditions of airways respiratory tract of human to the bottom of multiple breathing conditions.SudapornPoopra et al. [10] involved and experimented the PCL fluid velocities using asymptotic expansion as well as cilia's progress using Beaver-Joseph boundary condition in the porous medium.J. Prakash. Et al [11] perturbation technique experienced over a moving with the influence of chemical reactionon semiinfinite vertical plateat the time of mixed convection. R. Muthucumaraswamy [12] his problem discussed with uniform suction on regularly moving influence of a homogeneous first order chemical reaction in the vertical surface. Swetaprovo Chaudhuri et al. [13] established pandemic droplet evaporation and the breathing droplet direction using a determined physical norm mathematically. Jing Zhang et al. [14] analysed infected case report, who experience traumatic suffering from a vehicle accident and also persistCOVID-19,in the initial symptom with pleural effusion obtained. In the present study wedeal with new vision, how pleural fluid is contaminated due to novel corona virus occurrence of human respiratory tract with existing pulmonary disorders. Naturally lung has buoyancy effect. There may be no such reports had been determined in relevant literatures.

2. MATHEMATICAL FORMULATION

The substantial state of affairs can be written in the form of cartesian under the assumptions are based on study areas, we have considered an unsteady two-dimensional incompressible (Pleural Fluid), laminar glide of a viscous fluid uniform move phase h, fluid is double-dealing above and beneath bounded by porous layers. Initially time dependent slip boundary situation on the collocation of porous mediumat $t \le 0$, the location is thought to be, on the equal temperature Tand concentration C. Whilet > 0, the temperature of theplace is straight away accelerated to T_0 and concentration lifted to T_0 0 with recognize to time and maintained steady. Permit T_0 1 we have a long the fluid go with the flow and perpendicular to T_0 2. The physical situated diagram of the hassle is displayed below.

While deriving the governing equation, the following assumptions are made.

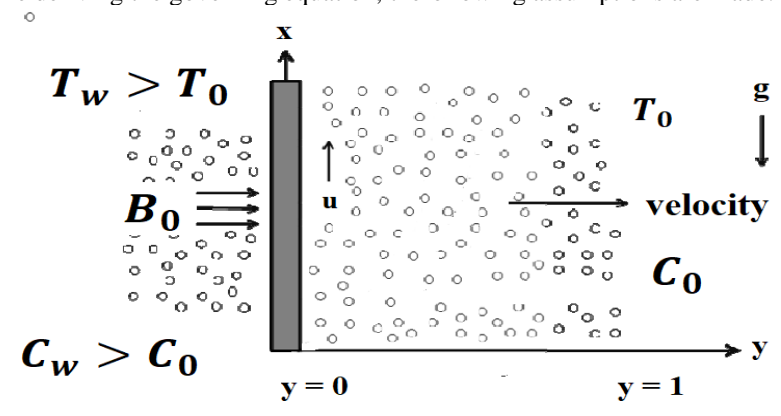


Fig .1 PhysicalConfiguration

ASSUMPTION:

- A uniform magnetic subject B₀ is applied in the y direction of the pleural fluidflow.
- Over the model, The Boussinesq approximation is applied.

- The density of contaminant pleural fluid isn't always consistent and the temperature between the debrisare uniform at some stage in the fluid movement due to buoyancy pressure.
- The gravitational force g, act towards vertical downward direction.
- The contaminant pathogens (COVID-19) are spherical (crown like position), non-undertaking, and equal in length and systematically disbursed in the fluid discharge place.

The Governing Equations are based on the proportion of Momentum, Mass, Energy SpeciesConcentrationas in J. Prakash et al. [11].

Equation of Continuity:

$$\frac{\partial \mathbf{u}}{\partial \mathbf{x}} + \frac{\partial \mathbf{v}}{\partial \mathbf{y}} = \mathbf{0} \tag{1}$$

Navier-stokes Equation:
$$\frac{\partial u}{\partial t} + u \frac{\partial u}{\partial x} + v \frac{\partial u}{\partial y} = -\frac{1}{\rho} \frac{\partial p}{\partial x} + v \left(\frac{\partial^2 u}{\partial x^2} + \frac{\partial^2 u}{\partial y^2} \right) + g \beta (T - T_0) + g \beta^* (C - C_0) - \frac{v}{k_1} u - \frac{\sigma B_0^2}{\rho} u - (2)$$

First law of thermodynamics Equation:
$$\rho C_p \left(\frac{\partial T}{\partial t} + u \frac{\partial T}{\partial x} + v \frac{\partial T}{\partial y} \right) = k_T \left(\frac{\partial^2 T}{\partial x^2} + \frac{\partial^2 T}{\partial y^2} \right) + j(T - T_0) \qquad \qquad \cdots \cdots (3)$$

where u and vare the velocity of the fluid particle, p known as fluid density, pknown as pressure,k₁known as permeability of the porous medium, gknown as gravitational acceleration, βknown volumetric coefficient of thermal expansion, β^* knownvolumetric coefficient of concentration expansion, ν known as kinematic viscosity, Tknown as temperature of the fluid, Toknown as initial temperature, Coknown asSpecific heat of the fluid at constant pressure, k_Tknown asThermal conductivity of the fluid, jknown as Heat absorption, Cknown as Concentration of the fluid, Dknown ascoefficient of Mass diffusivity of the fluid, Kcknownas Chemical Reaction Parameter.

The appropriate initial and boundary conditions under the assumptions, for Velocity involving moving fluid, Temperature and Concentration fields are defined as

When
$$\mathbf{t} = \mathbf{0}$$
, $\mathbf{u} = \mathbf{v} = \mathbf{0}$, $\mathbf{T} = \mathbf{T_0}$, $\mathbf{C} = \mathbf{C_0}$,

When $\mathbf{y} = \mathbf{0}$, $\mathbf{u} = \mathbf{v} = \mathbf{0}$, $\mathbf{T} = \mathbf{T_w} + \epsilon \, \mathbf{e}^{(\lambda t)} (\mathbf{T_w} - \mathbf{T_0})$, $\mathbf{C} = \mathbf{C_w} + \epsilon \, \mathbf{e}^{(\lambda t)} (\mathbf{C_w} - \mathbf{C_0})$ ------(6)

When $\mathbf{y} = \mathbf{1}$, $\mathbf{u} = \mathbf{1} + \epsilon \, \mathbf{e}^{(\lambda t)}$, $\mathbf{T_w} = \mathbf{T_0}$, $\mathbf{C_w} = \mathbf{C_0}$ -----(7)

Given problem by way of replacing the subsequent dimensionless quantities to reduce the many unknown

where, φ and θ are corresponding non-dimensional concentration and temperature respectively.

which implies $\mathbf{v} = \mathbf{v_0}(\mathbf{1} + \epsilon \mathbf{e}^{(\lambda t)})$, where $\mathbf{v_0}$ is a real positive constant additionally considered as the distinctive velocity order 1. Hence the fluid flow is two dimensional, in order to indeterminant length of the fluid region it clears that all of the physical quantities are independent of x -axis. (i.e.,) $\frac{\partial u}{\partial x} = 0$

After applying non-dimensional variables in basic governing Equations (1) to (4), neglecting the () symbol produce the equations are,

The initial & boundary condition making use of non-dimensional quantities becomes,

When
$$\mathbf{t}=\mathbf{0},\quad \mathbf{u}=\boldsymbol{\phi}=\boldsymbol{\theta}=\mathbf{0},$$
 When $\mathbf{y}=\mathbf{0},\quad \mathbf{u}=\mathbf{0}, \boldsymbol{\theta}=\boldsymbol{\phi}=\mathbf{1}+\boldsymbol{\varepsilon}\mathbf{e}^{(\lambda t)}$ ------(13) When $\mathbf{y}=\mathbf{1},\quad \mathbf{u}=\mathbf{1}+\boldsymbol{\varepsilon}\mathbf{e}^{(\lambda t)}, \boldsymbol{\theta}=\boldsymbol{\phi}=\mathbf{0}$ Where,

$$\begin{split} &Gr = \frac{g\beta\nu(T_W - T_0)}{\nu_0 ^3} \, [\, \, Grashof Number] & ; Gc = \frac{g\beta^*\nu(C_W - C_0)}{\nu_0 ^3} \, [\, \, Solutal Grashof Number] \\ &\sigma^* = \frac{\nu}{\nu_0 \sqrt{k_1}} \, \, [\, Porosity \, Parameter] \, \; ; H_a^{\ 2} = \frac{\sigma B_0^2 \nu}{\rho \nu_0^2} \, \, [\, Hartmann \, Number] \\ ⪻ = \frac{\mu C_p}{k_T} \, \, [\, Prandtl \, Number] & ; Sc = \nu/D \, \, [\, Schmidt \, Number] \\ &K = \frac{\nu K_c}{\nu_0^2} \, [\, Chemical \, Reaction \, Parameter] \; ; J = \frac{j\,\nu}{\nu_0^2} [\, Heat \, Absorption \, Parameter] \end{split}$$

SOLUTION METHOD

The set of arranged dimensionless equations from (9) to (12), as a way to set boundary conditions (13) can be used to find the analytic solution using perturbation method. This approach can be completed by depicting perturbation parameter ($\epsilon << 1$) is very very small flow velocity **u**, temperature θ and concentration φ followed as.

We proceeding our problem omitting higher order terms i.e., $o(\epsilon^2)$, substituting above equation into basic equations (9) to (12) to obtain following pair of equations are \mathbf{u}_0 , $\boldsymbol{\theta}_0$, $\boldsymbol{\phi}_0$ and \mathbf{u}_1 , $\boldsymbol{\theta}_1$, $\boldsymbol{\phi}_1$

Zero Order Equations: (ϵ^0)

In order to basic boundary conditions are,

To obtain zeroth-order velocity (u_0) , temperature (θ_0) , concentration (ϕ_0) , from (18) to (20) can be solved using boundary conditions (21). We get,

$$\left(\frac{d^2\theta_1}{dy^2}\right) - \Pr\left(\frac{d\theta_1}{dy} + (J\Pr - \lambda \Pr)\theta_1 = 0\right) \qquad -----(26)$$

$$\left(\frac{d^2 \varphi_1}{dy^2}\right) - \operatorname{Sc} \frac{d\varphi_1}{dy} - (\operatorname{K} \operatorname{Sc} + \lambda \operatorname{Sc})\varphi_1 = 0 \qquad -----(27)$$

In order to corresponding boundary conditions are,

Simultaneously to obtain first order velocity (u_1) , temperature (θ_1) , concentration (ϕ_1) , from (25) to (27) can be solved using boundary conditions (28). We get,

$$\begin{array}{l} u_1 = A_{11}\,e^{\,m_{11}y} + A_{12}\,e^{\,m_{12}y} - \left(\frac{1}{(e^{m_3} - e^{m_4})}\right)(R_3 + R_4) - \left(\frac{1}{(e^{m_7} - e^{m_8})}\right)(C_3 + C_4) - \cdots \\ \theta_1 = A_3\,e^{\,m_3y} + A_4\,e^{m_4y} \;\; (or) \\ \hline \\ \frac{e^{m_3y}(e^{\,m_3} - e^{\,m_4-1}) + e^{m_4y}}{(e^{m_3} - e^{m_4})} & - \cdots \end{array} \tag{30}$$

$$\phi_1 = A_7 \ e^{m_7 y} + A_8 e^{m_8 y} \ \ (or) \frac{e^{m_7 y} (e^{m_7 - e^{m_8 - 1}) + e^{m_8 y}}}{(e^{m_7 - e^{m_8})}} \qquad ------(31)$$

Employ complete solution of base and perturb parts are (22) to (24) and (29) to (31) in (14) to (17), we get final form of the solution is the summation of base partfactor and perturb element offers the corresponding Velocity, Temperature, Concentration of fluid molecule as given below:

$$\begin{split} T(\,y\,,\;t) = \,(\,\theta_0 \;\; + \,\varepsilon\,e^{\,(\lambda t)}\theta_1\,) \\ C(\,y\,,\;\;\;t) = \,(\,\phi_0 + \;\varepsilon\,e^{\,(\lambda t)}\phi_1\,) \end{split}$$

4. RESULTS AND DISCUSSION

The current observation is used to assess numerical computation of the analytic result for the subsequent fluid particles namely velocity, temperature, concentration distributions for numerous amounts of physical specification can express the characteristic of the fluid flow. Heat and Mass Transfer computed analytically also, their outcomeshave been portrayed graphically with the assist of MATLAB. Throughout the computation we employ corresponding values to classify the graph (t = 0.01, μ = 3 × 10⁻⁶; ρ = 992.2 × 10⁻¹⁵, g = 9.81 × 10⁶, λ = 0.3, ϵ = 0.01, Gr = 0.5, Gc = 0.5, Pr = 0.7, Sc = 0.60, σ^* = 0.2, K = 0.3, J = 0.0224, H_a = 0.3) SudapornPoopraet al. [10], excepting that the supplementary values of parameter kept as fixed state. We compute the various values of GrashofNumber, SolutalGrashof Number, Chemical Reaction Parameter, Hartmann Number, Porosity Parameter, Prandtl Number, Schmidt Number.

Effect of various parameters of Velocity distribution (U) with respect to y:

(i) Fig.2.Shows that various Effect of Magnetic range in the velocity distribution:
This force is known as Lorentz force. From the below graph, we understand that pleural fluid flow

of the Velocity decreases with increasing HARTMANN Number.

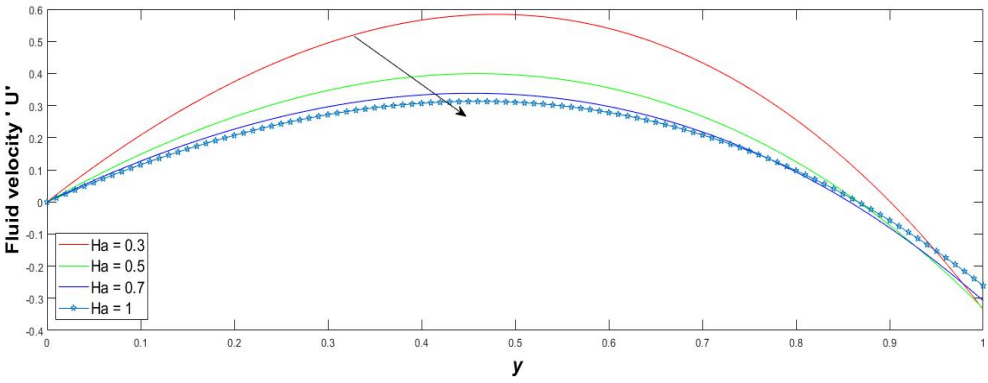


Fig.2 Velocity Field for different H_a.

(ii) Fig.3 shows that Effect of porosity parameter in the velocity distribution:

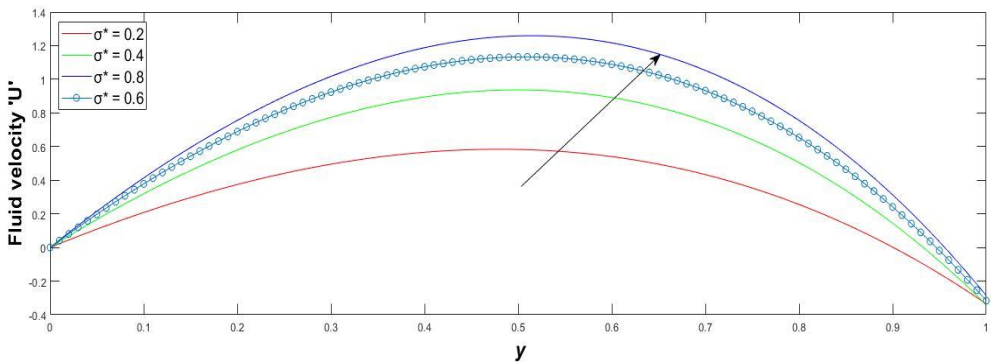


Fig.3 Velocity Field for different σ^{*2} .

Porosity describes a measure of the "Empty Space" in a solid material, its volume lies between 0 to 1. we perceived that velocity of the fluid increases with increasing Porosity permeable parameter (iii) Fig.4 shows that Effect of Grashof number in the velocity distribution:

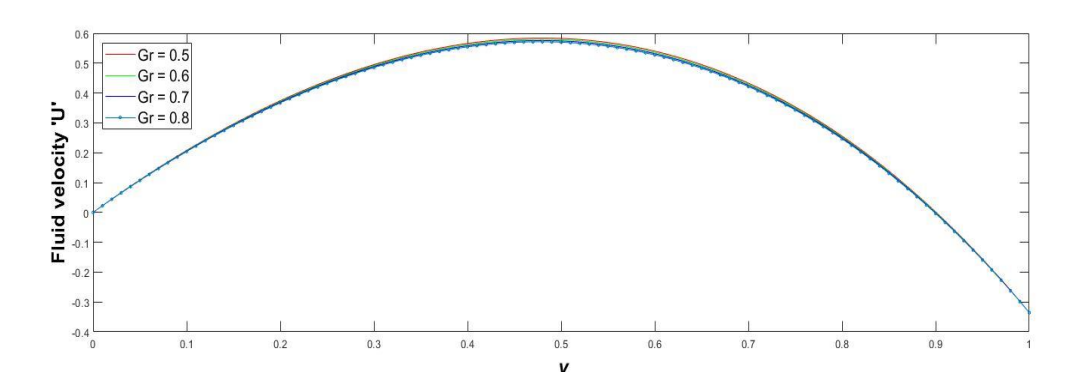


Fig. 4 Velocity Field for different Gr.Fig. 5 shows that Effect of SolutalGrashof number in the velocity distribution:

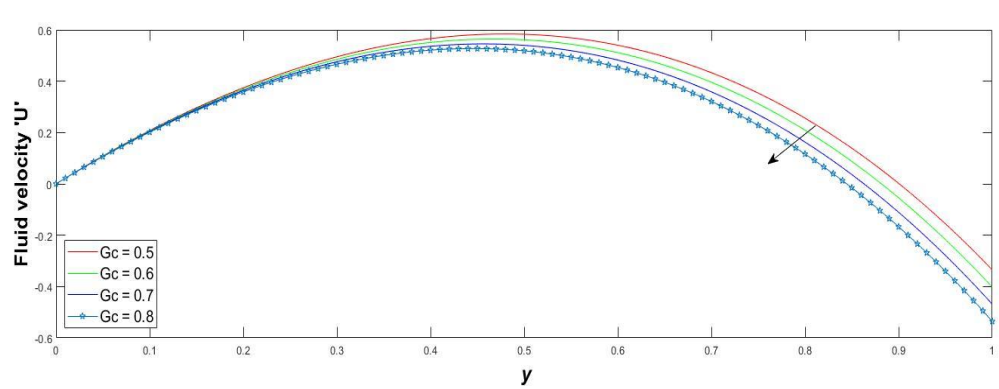


Fig.5 Velocity Field for different Gc.

(iv)

Above graphs are representing in the form of pictorially velocity of the pleural fluid decreases gradually while increasing Grashof and SolutalGrashof parameter values. It is clear that inside the lung, there is a buoyancy flow occurs during the fluid flow due to acceleration of gravitational force. It represents the domination of buoyancy force for the convection comparing to the viscous force. Buoyant force caused by a temperature gradient and concentration gradient. When the fluid is at rest two gradients would be absent. The variations of the Velocity are higher by the act of toxin (COVID -19) than fluid segment, while the solute attention of the solid particle adjustments. That is because of theexistence of COVID-19 contamination interior of the respiratory tract. It's miles clear that tremendous changes in the fluid Velocity havea major influence impact of contaminant particles when compared with pure fluid profile.

In addition, following remarks are made when temperature distributions are computed.

Effect of various parameters of Temperature distribution (T) with respect to y:

(v) Fig. 6 Shows that Effect of Prandtl Number in the Temperature distribution:

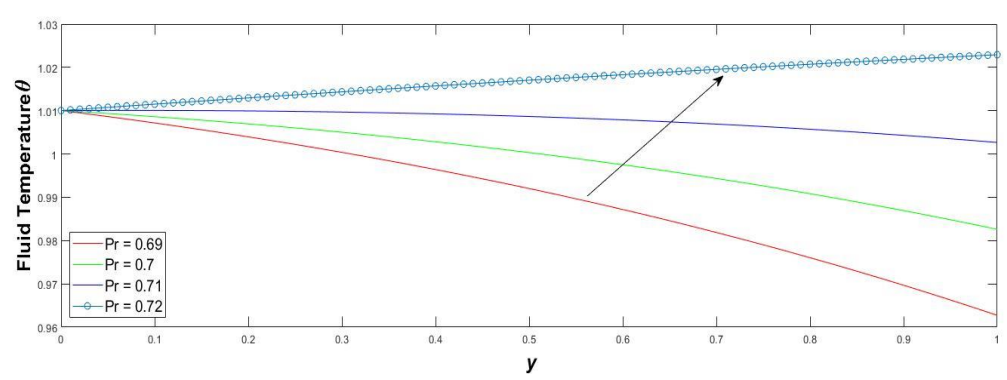


Fig.6 Temperature Field for different Pr.

The Prandtl Number restricts the relative density of the motion and thermal boundary layers. Also, it signifies the relative speed with which momentum and energy propagates through fluid. From this we observed that enhances Prandtl Number results increases in thermal boundary layersimultaneously Temperature increased inside the boundary layer.

(vi) Fig.7 Shows that Effect of Heat Absorption Parameter in the Temperature distribution:

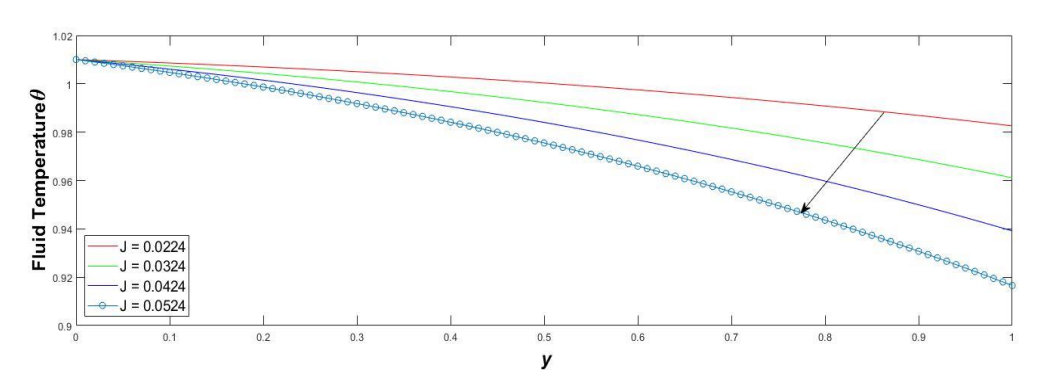


Fig.7 Temperature Field for different J.

Above graph displays temperature profile decreases with increasing Heat absorption parameter.

Effect of various parameters of Concentration distribution (C) with respect to y:

(vii) Fig.8 shows that Effect of numerousSchmidt Number in the Concentration distribution

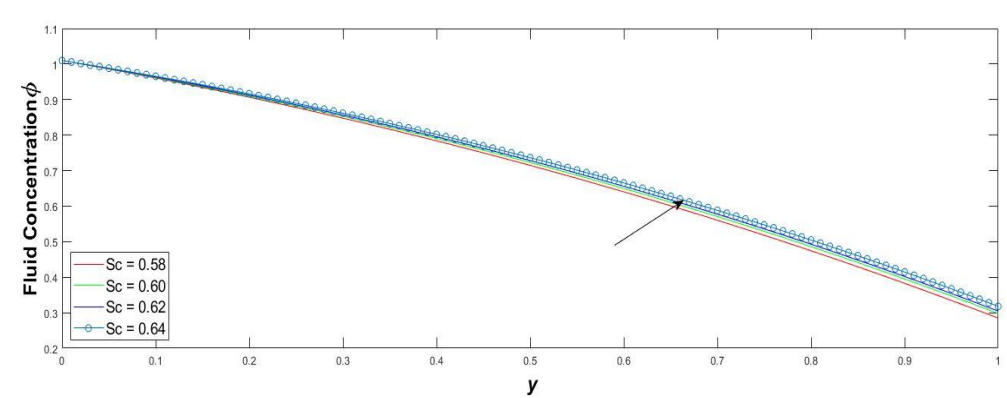


Fig.8 Concentration Field for different Sc.

(viii) Fig.9Shows that Effect of numerous Chemical Reaction parameter in the concentration distribution:

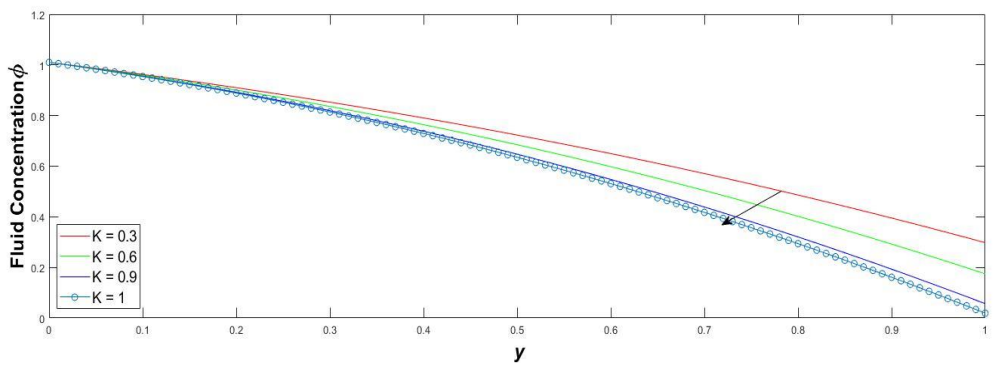


Fig.9ConcentrationField for different K.

Subsequently Concentration profile decreases of increasing Schmidt number and increases of Chemical reaction parameter. It shows that massive differences in COVID-19 diffusion rate by the reaction of chemical. The heat transfer rates increase and mass transfer decrease ultimately according to the nature of the fluid flow with increased buoyancy ratio.

CONCLUSION

The dimensionlessabove governing equations are solved analytically with the help of perturbation technique. We have concluded that heat and mass transfer on an unsteady magnetic field with natural convective flow of human respiratory tract due to buoyancy effect of lungs and chemical reaction inside the pleural cavity.

From the above results we summarized the major findings are given below:

- The velocity of a fluid flow decreases monotonically for increasing Hartmann number.
- Velocity of fluid flow decreases graduallyboth increasedGrashof and SolutalGrashofnumber.
- The velocity distribution increasing with moderate increased Porosity parameter.
- Temperatureof fluid flow increases due to increase in the thermal diffusion Prandtl number.
- Concentration profile increased due to increased Schmidt number.
- There is a significant fall due to increased Chemical reaction parameter and considerably reduces at prominent point.

6. APPENDIX

$$\begin{array}{lll} \textbf{6.} & \textbf{APPENDIX} \\ \textbf{Q} & = \textbf{H}_a^2 + \sigma^{*2} & ; & \textbf{S} = \textbf{J}.\textbf{Pr} & ; & \textbf{B} = \textbf{H}_a^2 + \sigma^{*2} + \lambda \\ \textbf{g}_1 & = \frac{\partial p_0}{\partial x} & ; & \boldsymbol{\omega} = \textbf{K}.\textbf{Sc} \\ \textbf{m}_1 & = \frac{(\textbf{Pr}) + \sqrt{(\textbf{Pr})^2 - 4 \cdot \textbf{JPr}}}{2} & ; & \boldsymbol{\omega} = \textbf{K}.\textbf{Sc} \\ \textbf{m}_1 & = \frac{(\textbf{Pr}) + \sqrt{(\textbf{Pr})^2 - 4 \cdot \textbf{JPr}}}{2} & ; & \boldsymbol{m}_2 & = \frac{(\textbf{Pr}) - \sqrt{(\textbf{Pr})^2 - 4 \cdot \textbf{JPr}}}{2} \\ \textbf{m}_3 & = \frac{(\textbf{Sc}) + \sqrt{(\textbf{Sc})^2 - 4 \cdot \textbf{KSc}}}{2} & ; & \boldsymbol{m}_4 & = \frac{(\textbf{Pr}) - \sqrt{(\textbf{Pr})^2 - 4 \cdot \textbf{JPr}}}{2} \\ \textbf{m}_5 & = \frac{(\textbf{Sc}) + \sqrt{(\textbf{Sc})^2 - 4 \cdot \textbf{KSc}}}{2} & ; & \boldsymbol{m}_4 & = \frac{(\textbf{Pr}) - \sqrt{(\textbf{Pr})^2 - 4 \cdot \textbf{JPr}}}{2} \\ \textbf{m}_7 & = \frac{(\textbf{Sc}) + \sqrt{(\textbf{Sc})^2 + 4 \cdot \textbf{Sc}} (\textbf{K} + \lambda)}{2} & ; & \boldsymbol{m}_4 & = \frac{(\textbf{Sc}) - \sqrt{(\textbf{Sc})^2 - 4 \cdot \textbf{JSc}}}{2} \\ \textbf{m}_7 & = \frac{(\textbf{Sc}) + \sqrt{(\textbf{Sc})^2 + 4 \cdot \textbf{Sc}} (\textbf{K} + \lambda)}{2} & ; & \boldsymbol{m}_{10} & = \frac{(\textbf{Sc}) - \sqrt{(\textbf{Sc})^2 + 4 \cdot \textbf{Sc}} (\textbf{K} + \lambda)}{2} \\ \textbf{m}_{11} & = \frac{1 + \sqrt{1 + 4 \left(\textbf{H}_a^2 + \sigma^{*2} + \lambda\right)}}{2} & ; & \boldsymbol{m}_{10} & = \frac{1 - \sqrt{1 + 4 \left(\textbf{H}_a^2 + \sigma^{*2} + \lambda\right)}}{2} \\ \textbf{m}_{11} & = \frac{1 + \sqrt{1 + 4 \left(\textbf{H}_a^2 + \sigma^{*2} + \lambda\right)}}{2} & ; & \boldsymbol{m}_{10} & = \frac{1 - \sqrt{1 + 4 \left(\textbf{H}_a^2 + \sigma^{*2} + \lambda\right)}}{2} \\ \textbf{m}_{11} & = \frac{1 - \sqrt{1 + 4 \left(\textbf{H}_a^2 + \sigma^{*2} + \lambda\right)}}{2} & ; & \boldsymbol{m}_{10} & = \frac{1 - \sqrt{1 + 4 \left(\textbf{H}_a^2 + \sigma^{*2} + \lambda\right)}}{2} \\ \textbf{m}_{11} & = \frac{1 - \sqrt{1 + 4 \left(\textbf{H}_a^2 + \sigma^{*2} + \lambda\right)}}}{2} & ; & \boldsymbol{m}_{10} & = \frac{1 - \sqrt{1 + 4 \left(\textbf{H}_a^2 + \sigma^{*2} + \lambda\right)}}{2} \\ \textbf{m}_{11} & = \frac{1 - \sqrt{1 + 4 \left(\textbf{H}_a^2 + \sigma^{*2} + \lambda\right)}}{2} & ; & \boldsymbol{m}_{10} & = \frac{1 - \sqrt{1 + 4 \left(\textbf{H}_a^2 + \sigma^{*2} + \lambda\right)}}{2} \\ \textbf{m}_{12} & = \frac{1 - \sqrt{1 + 4 \left(\textbf{H}_a^2 + \sigma^{*2} + \lambda\right)}}{2} & ; & \boldsymbol{m}_{10} & = \frac{1 - \sqrt{1 + 4 \left(\textbf{H}_a^2 + \sigma^{*2} + \lambda\right)}}{2} \\ \textbf{m}_{12} & = \frac{1 - \sqrt{1 + 4 \left(\textbf{H}_a^2 + \sigma^{*2} + \lambda\right)}}{2} & ; & \boldsymbol{m}_{10} & = \frac{1 - \sqrt{1 + 4 \left(\textbf{H}_a^2 + \sigma^{*2} + \lambda\right)}}{2} \\ \textbf{m}_{11} & = \frac{1 - \sqrt{1 + 4 \left(\textbf{H}_a^2 + \sigma^{*2} + \lambda\right)}}{2} & ; & \boldsymbol{m}_{10} & = \frac{1 - \sqrt{1 + 4 \left(\textbf{H}_a^2 + \sigma^{*2} + \lambda\right)}}{2} \\ \textbf{m}_{11} & = \frac{1 - \sqrt{1 + 4 \left(\textbf{H}_a^2 + \sigma^{*2} + \lambda\right)}}{2} & ; & \boldsymbol{m}_{10} & = \frac{1 - \sqrt{1 + 4 \left(\textbf{H}_a^2 + \sigma^{*2} + \lambda\right)}}{2} \\ \textbf{m}_{11} & = \frac{1 - \sqrt{1 + 4 \left(\textbf{H}_a^2 + \sigma^{*2} + \lambda\right)}}{2}$$

7. NOMENCLATURE

x - cartesian co - ordinate onward the portion

```
y – cartesian coordinate perpendicular to the portion
   u – dimensional velocity component u onward x directions
  v - dimensional velocity component u onward y directions
                  g - gravitational acceleration
                     p – pressure of the fluid
                         ρ – fluid density
             μ – dynamic viscosity of the pleural fluid
            v – kinematic viscosity of the pleural fluid
      k_1 – dimensional permeability of the porous medium
              \sigma- magnetic permeability of the fluid
                 B<sub>0</sub> - Coefficient of magnetic field
        \beta — Coefficient of volumetric thermal expansion
    \beta^* – Co – efficient of volumetric concentration expansion
               T - dimensional fluid temperature
              T_w – temperature of the surface wall
                     T_0 – Initial temperature
              C<sub>p</sub> - Specific heat at Cnstant pressure
                    K<sub>T</sub> − thermal conductivity

    Coefficient of spatial heat absorption

               C - Dimensional fluid Concentration
               C<sub>w</sub> - Concentration of the suface wall
                     C<sub>0</sub> – Initial concentration
                       D - Mass diffusivity
                K - Chemical Reaction Parameter
                       Gr - Grashof Number
                   Gc - Solutal Grashof Number
                     H<sub>a</sub> – Hartmann Number
                       Pr - Prandtl Number
                       Sc - Schmidt Number
                      \sigma^* – Porosity Parameter
```

ACKNOWLEDGMENT

This author grateful to the arbitrator for their constructive suggestions and valuable comments, which undoubtedly improved the earlier version of the manuscript.

REFERENCES

- Zahra Ahmadinejad, Faeze Salah hour, Omid Dadras, Hesan Rezaei, Syyed Ahmad Alinaghi, "Pleural Effusion as a Sign of Coronavirus Disease 2019 (COVID-19) Pneumonia: A Case Report". Journal of Infectious Disorders - Drug TargetsDOI: <u>10.2174/1871526520666200609125045</u>
- 2. Saffman.P.G., (1962). On the stability of laminar flow of a dusty gas. J.Fluid Mech, 13, 120-134.
- 3. Adrian Bejan, R. and Khair, Heat and mass transfer by natural convection in a porous medium, Int. J.Heat Mass Transfer, 28 (1985) 909-918.
- 4. R. Mittal, R. Ni and J.-H. Seo, The flow physics of COVID-19, J. Fluid Mech. (2020), vol. 894, F2.
- 5. S. Das, R. N. Jana and A. J. Chamkha, Unsteady Free Convection Flow past a Vertical Plate with Heat and Mass Fluxes in the Presence of Thermal Radiation, Journal of Applied Fluid Mechanics, Vol. 8, No. 4, pp. 845-854, 2015.
- Christian J. Roth, Lena Yoshihara, Mahmoud Ismail, Wolfgang A. Wall, Computational modelling of the respiratory system: Discussion of coupled modelling approaches and two recent extensions, Journal of Comput. Methods Appl. Mech. Engg. 314 (2017) 473

 –493.
- 7. Richard Haber James B. Grotberg, Matthew R. Glucksberg, GiuseppeMiserocchi Daniele Venturoli, Massimo Del Fabbro, Christopher M. Waters, Steady-State Pleural Fluid Flow and Pressure and the Effects of Lung Buoyancy, J. of Biomechanical Engineering OCTOBER (2001) Vol. 123, 485-492.
- 8. G. V. Ramana Reddy, Ch. V. Ramana Murthy, and N. Bhaskar Reddy, Unsteady MHD Free Convective Mass Transfer Flow Past an Infinite Vertical Porous Plate with Variable Suction and Soret Effect, Int. J. of Appl. Math and Mech. 7 (21): 70-84, 2011.

- 9. T. B. Martonen, Z. Zhang & R. C. Lessmann, Fluid Dynamics of the Human Larynx and Upper Tracheobronchial Airways, Aerosol Science and Technology 193133-156 (1993). DOI: 10.1080/02786829308959627
- 10. SudapornPoopra andKanognudgeWuttanachamsri,The Velocity of PCL Fluid in Human Lungs with Beaver and Joseph Boundary Condition by Using Asymptotic Expansion Method, www.mdpi.com/journal/mathematics, 2019, 7, 567; doi:10.3390/math7060567.
- 11. J. Prakash, R. Sivaraj& B. Rushi Kumar, Influence of chemical reaction on unsteady MHD mixed convective flow over a moving vertical porous plate, International Journal of Fluid Mechanics 3(1) (2011) 1-14.
- 12. R.Muthucumaraswamy, Effects of a chemical reaction on a moving isothermal vertical surface with suction, Acta Mechanica, 155, March -(2002) 65-70.
- 13. Swetaprovo Chaudhuri, Saptarshi Basu, Prasenjit Kabi, Vishnu R. Unni, and Abhishek Saha, Modelling the role of respiratory droplets in Covid-19 type pandemics. Journal Physics of Fluids 32, 063309 (2020); https://doi.org/10.1063/5.0015984.
- 14. Jing Zhang, Chunwei Chai, Lifang Li, Mengrui Qu, HuipingDuan, Liping Ren, Hui Zhao, COVID-19 with pleural effusion as the initial symptom: a case study analysis. Ann Palliat Med 2020;9(5):3710-3715; http://dx.doi.org/10.21037/apm-20-1720.
- 15. Asraf Yasmin, B., Latha, R., & Manikandan, R. (2019). Implementation of Affective Knowledge for any Geo Location Based on Emotional Intelligence using GPS. International Journal of Innovative Technology and Exploring Engineering, 8(11S), 764–769. https://doi.org/10.35940/ijitee.k1134.09811s19
- 16. Muruganantham Ponnusamy, Dr. A. Senthilkumar, & Dr.R.Manikandan. (2021). Detection of Selfish Nodes Through Reputation Model In Mobile Adhoc Network MANET. Turkish Journal of Computer and Mathematics Education, 12(9), 2404–2410. https://turcomat.org/index.php/turkbilmat/article/view/3720